ELSEVIER

Materials Science and Engineering A 454–455 (2007) 379–383

MATERIALS SCIENCE & ENGINEERING A

www.elsevier.com/locate/msea

Internal friction of B2 → B19′ martensitic transformation of $Ti_{50}Ni_{50}$ shape memory alloy under isothermal conditions

S.H. Chang, S.K. Wu *

Department of Materials Science and Engineering, National Taiwan University, Taipei 106, Taiwan

Received 7 September 2006; received in revised form 7 November 2006; accepted 23 November 2006

Abstract

The inherent internal friction $(IF_{PT} + IF_I)_{B2\rightarrow B19'}$ of cold-rolled and annealed $Ti_{50}Ni_{50}$ alloy that exhibits B2 → B19′ martensitic transformation is studied under isothermal conditions. The tan δ value of $(IF_{PT} + IF_I)_{B2\rightarrow B19'}$ is proportional to $\sigma_0/\nu^{1/2}$ and its damping mechanism is thus related to stress-assisted martensitic transformation and stress-assisted motion of twin boundaries. The tan δ value of $(IF_{PT} + IF_I)_{B2\rightarrow B19'}$ is smaller than those of $(IF_{PT} + IF_I)_{B2\rightarrow R}$ and $(IF_{PT} + IF_I)_{R\rightarrow B19'}$ because the former shows no R-phase. The obliterated dislocations and defects after sufficient annealing can lower the tan δ value of the relaxation peak at about −60 °C.

Keywords: TiNi shape memory alloy; Martensitic transformation; Internal friction; Dynamic mechanical analysis

1. Introduction

TiNi-based alloys exhibiting a thermoelastic martensitic transformation are known as very important shape memory alloys (SMAs) with a good shape memory effect (SME) and superelasticity [1]. Many reported studies revealed that TiNi SMAs perform a high level of mechanical damping and are suitable for energy dissipation applications [2–10]. Near equiatomic TiNi SMAs exhibit high internal friction peaks in the temperature range of martensitic transformation and the magnitude of these internal friction peaks are associated with experimental parameters, such as temperature heating/cooling rate ($\dot{T}$), frequency (ν) and amplitude (σ_0) [3]. In addition to the internal friction peaks associated with martensitic transformation, the high damping property is also obtained in the R-phase and B19′ martensite due to the easy movement of their own twin boundaries [5]. Moreover, it has also been reported that a suitable control of the annealing conditions of cold-rolled TiNi SMAs can acquire a rather good damping capacity [10].

The internal friction of a first-order phase transformation is proposed to be decomposed into three terms: IF_{Tr}, IF_{PT} and IF_I [11–14]. The first term IF_{Tr} is a transitory internal friction, which appears only at low ν and non-zero $\dot{T}$. The second term IF_{PT} is the internal friction due to phase transformation, but it does not depend on $\dot{T}$. The third term IF_I is the intrinsic internal friction of austenitic or martensitic phase and depends strongly on microstructure properties, such as dislocations, vacancies and twin boundaries.

All the aforementioned reports focus on the studies involving damping characteristics of transitory internal friction (IF_{Tr}); however, only a few works discuss the inherent internal friction ($IF_{PT} + IF_I$) during martensitic transformation and/or the intrinsic internal friction (IF_I) of a single phase measured under isothermal treatment in TiNi-based SMAs. Chang and Wu [15] reported that the inherent internal friction during B2 → R and R → B19′ martensitic transformation, i.e., $(IF_{PT} + IF_I)_{B2\rightarrow R}$ and $(IF_{PT} + IF_I)_{R\rightarrow B19'}$, are both linearly proportional to $\sigma_0/\nu^{1/2}$ and their damping mechanism is mainly generated from the stress-assisted martensitic transformation and stress-assisted motions of twin boundaries. They also showed that the intrinsic internal friction IF_I of the R-phase and B19′ martensite is composed of static internal friction (IF_S) and dynamic internal friction (IF_D) [16]. The tan δ values of IF_S in both R-phase and B19′ martensite are proportional to $\sigma_0/\nu^{1/2}$ and are related to the stress-assisted motions of twin boundaries. However, the damping characteristic of TiNi SMAs exhibited one-stage B2 → B19′ martensitic transformation under isothermal conditions has not been systematically investigated. In this study, equiatomic TiNi SMA was severely cold-rolled and then annealed at 650 °C for 30 min to obtain a one-stage B2 → B19′ transformation in cooling.

* Corresponding author. Tel.: +886 2 2363 7846; fax: +886 2 2363 4562.
E-mail address: skw@ntu.edu.tw (S.K. Wu).

0921-5093/$ – see front matter © 2006 Elsevier B.V. All rights reserved.
doi:10.1016/j.msea.2006.11.157

The tan δ and storage modulus E_0 values of the specimen were measured by the dynamic mechanical analyzer (DMA) under isothermal conditions at different temperatures. Thereafter, the isothermal damping characteristic of $(IF_{PT} + IF_I)_{B2\rightarrow B19'}$ at one-stage B2 → B19′ martensitic transformation is compared with those of $(IF_{PT} + IF_I)_{B2\rightarrow R}$ and $(IF_{PT} + IF_I)_{R\rightarrow B19'}$ at two-stage B2 → R → B19′ martensitic transformation.

2. Experimental procedures

Equiatomic TiNi SMA was prepared by conventional vacuum arc re-melting. The as-melted ingot was hot-rolled at 850 °C into a 2-mm-thick plate and the plate was subsequently solution-treated at 850 °C for 2 h followed by quenching in water. Then, the plate was cold-rolled at room temperature along the hot-rolling direction and reached a final reduction of 30% thickness. No annealing was conducted during cold-rolling so to avoid the occurrence of recrystallization. Thereafter, the cold-rolled plate was cut into test specimens, sealed in an evacuated quartz tube and annealed at 650 °C for 30 min. Transformation temperatures of cold-rolled and annealed specimens were determined by differential scanning calorimetry (DSC) test using TA Q10 DSC equipment. The weight of the specimen used in DSC was about 30 mg and the heating and cooling rates were set at 10 °C/min. Specimens for DMA experiment were cut to the dimension of 40 mm × 5 mm × 1.26 mm along the rolling direction to eliminate the influence of rolling texture [17]. tan δ and E_0 values were measured by TA 2980 DMA equipment with $\dot{T} = 3\,^{\circ}C/\,min$, $\nu = 1$ Hz and $\sigma_0 = 5\,\mu m$. The inherent damping characteristics of the specimens were also investigated by DMA, but now measured under isothermal conditions at different temperatures. The detailed procedure for the isothermal DMA test was conducted as follows. The specimen was initially cooled starting from 150 °C at a cooling rate of 3 °C/min and was kept isothermally for 30 min at the set temperature. After being isothermal for 30 min, the specimen was heated to 150 °C to ensure that it had returned to the B2 parent phase. Then, the specimen was cooled to another set temperature and kept isothermally at that temperature for 30 min, and so on. Under the isothermal condition, the set temperature was chosen within the range of +80 to −80 °C.

3. Results and discussion

3.1. DSC and DMA measurements at constant $\dot{T}$

Fig. 1(a and b) shows DSC and DMA curves, respectively, of 30% cold-rolled $Ti_{50}Ni_{50}$ alloy annealed at 650 °C for 30 min. As seen in Fig. 1(a), there is a B2 → B19′ transformation peak in the forward transformation and a B19′ → B2 one in the reverse. Fig. 1(b) illustrates the tan δ and E_0 curves of the specimen of Fig. 1(a). Only the cooling curves with $\dot{T} = 3\,^{\circ}C/\,min$, $\nu = 1$ Hz and $\sigma_0 = 5\,\mu m$ are shown in Fig. 1(b). There is also a B2 → B19′ internal friction peak appearing in the tan δ curve which corresponds to the observed peak in the DSC curve shown in Fig. 1(a). Also seen in Fig. 1(b), the E_0 curve decreases gently in the B2 parent phase, and then reaches a minimum during B2 → B19′ martensitic transformation. After B2 → B19′ martensitic transformation is completed, the E_0 value in B19′ martensite increases with decreasing temperature. The peak temperatures measured by DSC and DMA tests show a small shift due to different cooling rates and specimen sizes. Except for the aforementioned tan δ transformation peak, an extra broad peak is also observed in Fig. 1(b) at about −75 °C. This extra peak is known as the relaxation peak [4], and is not observed in the DSC curve.

3.2. DMA measurement under isothermal conditions

Fig. 2 plots the tan δ values versus isothermal interval when the specimen of Fig. 1 is isothermal-treated at 80 °C (B2 parent phase), 20 °C (B2 → B19′ transformation peak) and −80 °C (B19′ martensite) for 0–30 min. In Fig. 2, the tan δ value measured at B2 → B19′ transformation decreases drastically with increasing isothermal interval and reaches a steady value after 10–15 min. The decayed tan δ value as a result of isothermal treatment represents the transitory internal friction of B2 → B19′ transformation, $(IF_{Tr})_{B2\rightarrow B19'}$, which is associated with the magnitude of $\dot{T}$. The steady tan δ value after 15 min of isothermal treatment shown in Fig. 2 indicates the inherent internal friction $(IF_{PT} + IF_I)_{B2\rightarrow B19'}$ during phase transformation which is independent of $\dot{T}$. Moreover, as seen in Fig. 2, the measured tan δ values of the B2 parent phase are almost the same throughout the entire isothermal duration, while the

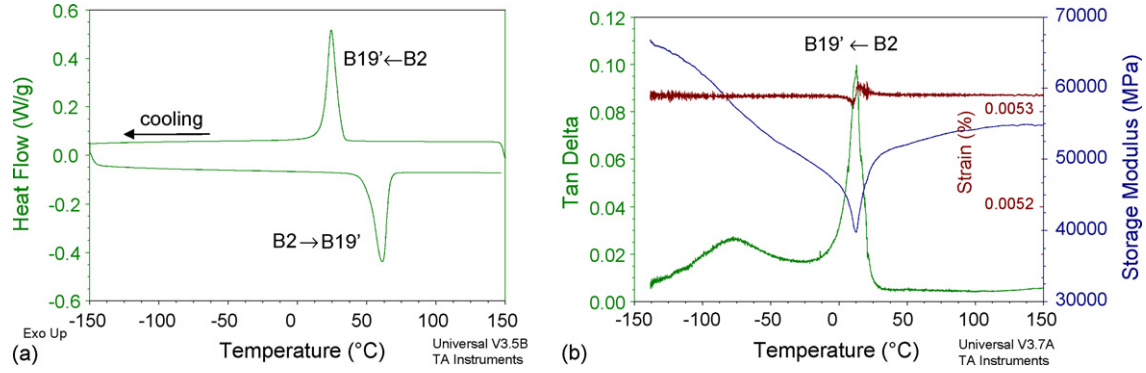

Fig. 1. (a) DSC curves measured at $\dot{T} = 10\,^{\circ}C/\,min$ and (b) tan δ and storage modulus E_0 curves measured at $\dot{T} = 3\,^{\circ}C/min$, $\nu = 1$ Hz and $\sigma_0 = 5\,\mu m$ for 30% cold-rolled $Ti_{50}Ni_{50}$ alloy annealed at 650 °C for 30 min.

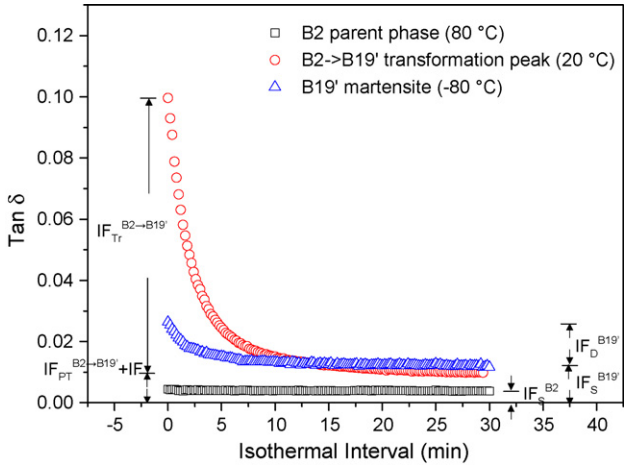

Fig. 2. tan δ values vs. isothermal interval for Fig. 1 specimen measured at $\nu = 1$ Hz, $\sigma_0 = 5$ μm and isothermal at 80 °C (B2 parent phase), 20 °C (B2 → B19′ transformation peak) and −80 °C (B19′ martensite phase) for 0–30 min.

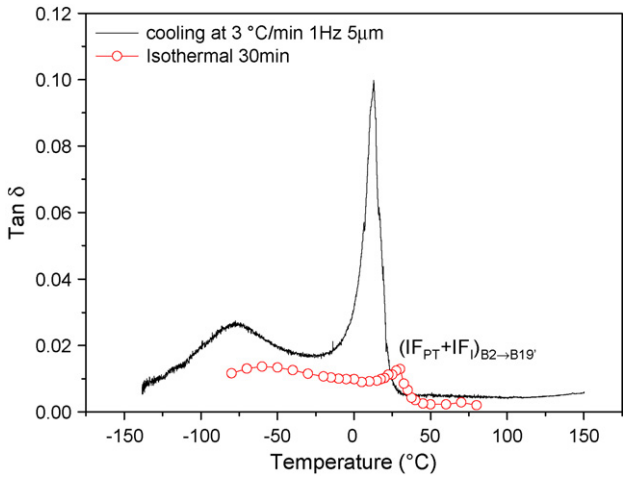

Fig. 3. tan δ values vs. temperature for Fig. 1 specimen measured at $\nu = 1$ Hz, $\sigma_0 = 5$ μm. The solid curve is measured at $\dot{T} = 3$ °C/min and the empty circle curve is the data of the specimen kept isothermal for 30 min.

measured tan δ values of B19′ martensite decrease with increasing isothermal interval and reaches a steady value after 10 min. As illustrated in Fig. 2, the tan δ value of B19′ martensite is composed of a dynamic term $IF_D^{B19'}$, which diminishes during isothermal condition and a static term $IF_S^{B19'}$, which is the steady value measured after 30 min of isothermal treatment [16].

In order to investigate the damping characteristics of $(IF_{PT} + IF_I)_{B2\rightarrow B19'}$, DMA test under 30-min isothermal treatment at different temperatures was conducted and the results are indicated in Fig. 3. The tan δ curve of Fig. 1(b) (measured at $\dot{T} = 3$ °C/min) is also plotted in Fig. 3 for comparison. When the isothermal temperature is set at about 30 °C, an inherent internal friction peak of $(IF_{PT} + IF_I)_{B2\rightarrow B19'}$ appears with a tan δ value of 0.013. The temperature shift between the $(IF_{PT} + IF_I)_{B2\rightarrow B19'}$ peak of Fig. 3 and the B2 → B19′ internal friction peak of Fig. 1(b) is due to the cooling rate effect. This cooling rate effect can be considered as a technical effect which corresponds to the large specimen and big furnace size used in DMA. Fig. 4(a and b) shows the measured tan δ values of $(IF_{PT} + IF_I)_{B2\rightarrow B19'}$ peak under isothermal conditions at different σ_0 and ν, respectively. As illustrated in Fig. 4, the tan δ value of $(IF_{PT} + IF_I)_{B2\rightarrow B19'}$ peak is linearly proportional to σ_0 and $1/\nu^{1/2}$ when the applied ν and σ_0 are within 10 Hz and 15 μm, respectively. This feature is similar to the damping characteristics of $(IF_{PT} + IF_I)_{B2\rightarrow R}$ and $(IF_{PT} + IF_I)_{R\rightarrow B19'}$ at two-stage B2 → R → B19′ martensitic transformation [15]. Therefore, the damping mechanism of $(IF_{PT} + IF_I)_{B2\rightarrow B19'}$ can also be attributed to the stress-assisted martensitic transformation and stress-assisted motions of the twin boundary in B19′ martensite. As shown in Fig. 2, the tan δ value of static internal friction in B19′ martensite ($IF_S^{B19'}$) is much higher than that in the B2 parent phase (IF_S^{B2}). IF_S^{B2} exhibits a rather small tan δ value because it comes only from the dynamic/static hysteresis of lattice defects. On the other hand, $IF_S^{B19'}$ has a higher tan δ value because of its abundant twin boundaries in between the variants which can be easily moved by the external stress to accommodate the applied strain [16]. With further isothermal treatment at lower temperatures, the tan δ value of intrinsic internal friction also exhibits a relaxation peak at around −60 °C, as shown in Fig. 3.

3.3. Comparison of damping characteristics between B2 → B19′ and B2 → R → B19′ martensitic transformation

Fig. 5(a and b) shows the tan δ and E_0 values, respectively, of the specimens annealed at 650 °C for 2 min [15]

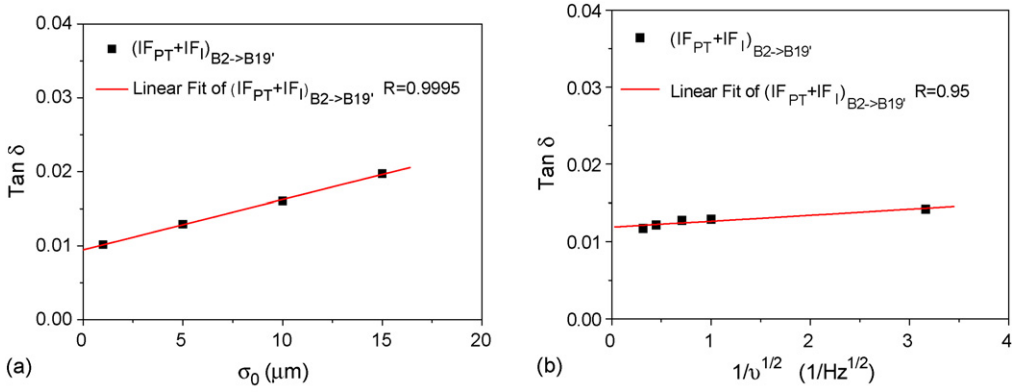

Fig. 4. tan δ values of $IF_{PT}^{B2\rightarrow B19'} + IF_I$ measured after isothermal at inherent internal friction peak as a function of: (a) σ_0 and (b) $1/\nu^{1/2}$.

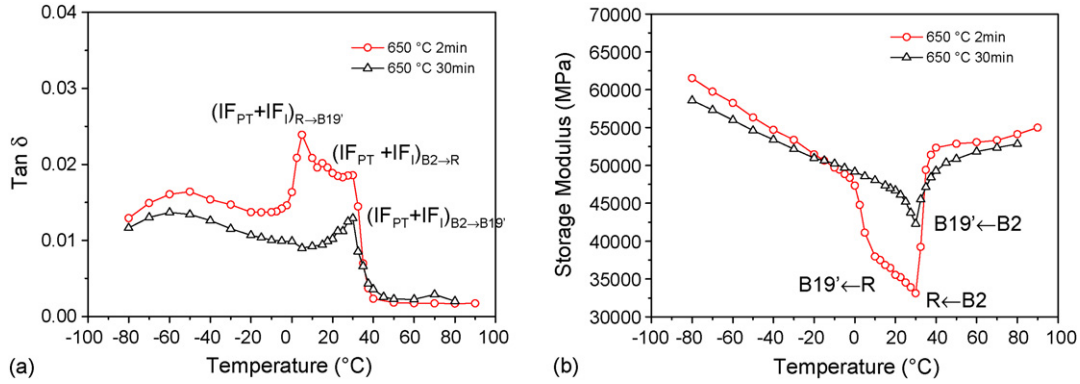

Fig. 5. (a) tan δ and (b) E_0 values of the specimen annealed at 650 °C for 2 min [15] and 30 min measured after isothermal 30 min at different temperatures.

and 30 min (from Fig. 3) after 30-min isothermal treatment at different temperatures. The experimental parameters used for these two specimens in Fig. 5 are $\nu = 1$ Hz and $\sigma_0 = 5$ μm. As seen in Fig. 5(a), the specimen annealed at 650 °C for 2 min exhibits B2 → R and R → B19′ inherent internal friction peaks, $(IF_{PT} + IF_I)_{B2\rightarrow R}$ and $(IF_{PT} + IF_I)_{R\rightarrow B19'}$, while the specimen annealed at 650 °C for 30 min shows only a single B2 → B19′ inherent internal friction peak, $(IF_{PT} + IF_I)_{B2\rightarrow B19'}$, in cooling. Meanwhile, as shown in Fig. 5(a), tan δ values of both $(IF_{PT} + IF_I)_{B2\rightarrow R}$ and $(IF_{PT} + IF_I)_{R\rightarrow B19'}$ are higher than that of $(IF_{PT} + IF_I)_{B2\rightarrow B19'}$. As shown in Fig. 5(b), the E_0 value of the specimen annealed at 650 °C for 2 min decreases drastically and shows a deep minimum (about 33,000 MPa) associated with B2 → R transformation and a shallow minimum (about 37,500 MPa) related to R → B19′ transformation. On the other hand, the E_0 value of the specimen annealed at 650 °C for 30 min also decreases at B2 → B19′ martensitic transformation but shows a E_0 minimum value of about 42,300 MPa. The lower E_0 minimum value in B2 → R and R → B19′ transformations than that in B2 → B19′ implies that the specimen becomes more softened as the R-phase is formed. This feature indicates that the formation of R-phase can induce easier movement of twin boundaries and more dissipated energy under constant stress amplitude [10], thus exhibiting a higher tan δ value of IF_I. Consequently, the tan δ value of $(IF_{PT} + IF_I)_{B2\rightarrow B19'}$ is smaller than those of $(IF_{PT} + IF_I)_{B2\rightarrow R}$ and $(IF_{PT} + IF_I)_{R\rightarrow B19'}$ because the R-phase is not formed in the former.

In addition to inherent internal friction, the static internal friction $IF_S^{B19'}$ of the specimen annealed at 650 °C for 2 min is also larger than that annealed at 650 °C for 30 min, as shown in Fig. 5(a). However, as shown in Fig. 5(b), the E_0 values of B19′ martensite in these two specimens are not significantly different. This phenomenon reveals that the difference in tan δ values of $IF_S^{B19'}$ between these two specimens is not due to the different mobility of twin boundaries in B19′ martensite, but comes from the different magnitude of the relaxation peak. As shown in Fig. 5(a), the specimen annealed at 650 °C for 2 min shows a transformation sequence of B2 → R → B19′ because this specimen has abundant residual tangled dislocations and defects which induce the formation of the R-phase. On the other hand, the specimen annealed at 650 °C for 30 min has tangled dislocations and defects to be annihilated and only B2 → B19′ transformation can be obtained [18–20]. It has been reported that the relaxation peak in TiNi alloys near 200 K is originated from the movement of dislocations that have been pinned by point defects [2,21]. Therefore, the lower tan δ value of the relaxation peak in the specimen annealed at 650 °C for 30 min can be expected owing to the obliterated dislocations and defects after sufficient annealing in this specimen.

4. Conclusions

The tan δ value of inherent internal friction $(IF_{PT} + IF_I)_{B2\rightarrow B19'}$ corresponding to B2 → B19′ transformation of $Ti_{50}Ni_{50}$ SMA is linearly proportional to $\sigma_0/\nu^{1/2}$ when the applied ν and σ_0 are within 10 Hz and 15 μm, respectively. This characteristic explicates that the damping mechanism of $(IF_{PT} + IF_I)_{B2\rightarrow B19'}$ is mainly generated from the stress-assisted martensitic transformation and stress-assisted motion of twin boundaries. $IF_S^{B19'}$ have higher tan δ values than those of IF_S^{B2} because of the abundant twin boundaries present in between the B19′ variants, which can be easily moved by the external stress to accommodate the applied strain. The E_0 minimum values of B2 → R and R → B19′ martensitic transformations under isothermal treatment are lower than those of B2 → B19′ transformation. At the same time, the tan δ values of $(IF_{PT} + IF_I)_{B2\rightarrow R}$ and $(IF_{PT} + IF_I)_{R\rightarrow B19'}$ are higher than those of $(IF_{PT} + IF_I)_{B2\rightarrow B19'}$. These features come from the fact that the R-phase is not formed in the latter. The lower tan δ value of the relaxation peak in the specimen annealed at 650 °C for 30 min than that in the specimen annealed at 650 °C for 2 min is attributed to the obliterated dislocations and defects after sufficient annealing of the former.

Acknowledgement

The authors gratefully acknowledge the financial support for this research provided by the National Science Council (NSC), Taiwan, Republic of China, under Grants Nos. NSC95-2221-E002-164.

References

[1] C.M. Wayman, T.W. During, in: T.W. During, K.N. Melton, D. Stöckel, C.M. Wayman (Eds.), Engineering Aspects of Shape Memory Alloys, Butterworth-Heinemam, London, 1990, pp. 3–20.
[2] K. Iwasaki, R. Hasiguti, Trans. JIM 28 (1987) 363.
[3] O. Mercier, K.N. Melton, Y. De Préville, Acta Metall. 27 (1979) 1467.
[4] S.K. Wu, H.C. Lin, T.S. Chou, Acta Metall. 38 (1990) 95.
[5] H.C. Lin, S.K. Wu, M.T. Yeh, Metall. Mater. Trans. A 24 (1993) 2189.
[6] K. Sugimoto, T. Mori, K. Otsuka, K. Shimizu, Scripta Metall. 8 (1974) 1341.
[7] Y. Liu, J. Van Humbeeck, R. Stalmans, L. Delaey, J. Alloys Compd. 247 (1997) 115.
[8] B. Coluzzi, A. Biscarini, R. Campanella, L. Trotta, G. Mazzolai, A. Tuissi, F.M. Mazzolai, Acta Mater. 47 (1999) 1965.
[9] S.K. Wu, H.C. Lin, J. Alloys Compd. 72-78 (2003) 355.
[10] S.H. Chang, S.K. Wu, Key Eng. Mater. 319 (2006) 9.
[11] J.F. Delorme, R. Schmid, M. Robin, P. Gobin, J. Phys. 32 (1971) C2–101.
[12] W. Dejonghe, R. De Batist, L. Delaey, Scripta Metall. 10 (1976) 1125.
[13] J.E. Bidaux, R. Schaller, W. Benoit, J. Phys. 46 (1985), C10-601.
[14] J. Van Humbeek, J. Stoiber, L. Delaey, R. Gotthardt, Z. Metalkd. 86 (1995) 1976.
[15] S.H. Chang, S.K. Wu, Scripta Mater. 55 (2006) 311.
[16] S.H. Chang, S.K. Wu, Internal friction of R-phase and B19′ martensite in equiatomic TiNi shape memory alloy under isothermal consitions, J. Alloys Compd. (2006), doi:10.1016/j.jallcom.2006.07.092.
[17] S.H. Chang, S.K. Wu, Scripta Mater. 50 (2004) 937.
[18] Y. Liu, P.G. McCormick, Acta Metall. Mater. 42 (1994) 2401.
[19] F. Khelfaoui, G. Guénin, Mater. Sci. Eng. A 355 (2003) 292.
[20] S.H. Chang, S.K. Wu, G.H. Chang, Mater. Sci. Eng. A 438-440 (2006) 509.
[21] J.S. Zhu, R. Schaller, W. Benoit, Phys. Lett. A 141 (1989) 177.